Journal of
Materials Chemistry A
Materials for energy and sustainability

Supporting Information

Controlled Mechanical Cleavage of Bulk Niobium Diselenide to Nanoscaled Sheet, Rod, and Particles Nanostructures for Pt-free Dye-sensitized Solar Cells

By Mohammed Aziz Ibrahem, Wei-Chih Huang Tian-wey Lan, Karunakara Moorthy Boopathi, Yu-Chen Hsiao, Chih-Han Chen, Widhya Budiawan, Yang-Yuan Chen, Chia-Seng Chang, Lain-Jong Li Chih-Hung Tsai,* and Chih Wei Chu*

Coresponding authers:

Dr. Chih-Hung Tsai, Department of Opto-Electronic Engineering, National Dong Hwa University, Hualien 97401, Taiwan, e-mail: cht@mail.ndhu.edu.tw
Dr. Chih Wei Chu, RCAS, Academia Sinica, Taipei 115, Taiwan, e-mail: gchu@gate.sinica.edu.twa

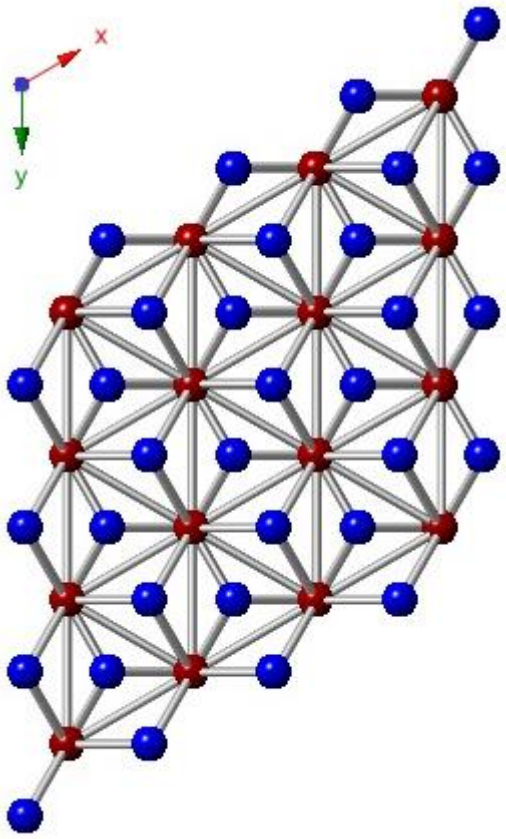

Figure S1.Crystal structure model of $NbSe_2$: The (001) section of the crystal structure model of the $NbSe_2$ supercell; blue and red balls represent Se and Nb atoms, respectively. Six equivalent Nb–Se distances are found within the trigonal prism around Nb. The calculated lattice constants ($a = b = 3.0$ Å ; $c = 12.547$ Å) are consistent with the standard data recorded in CPDS 01-089-4313.

S1 Scale-up:

This method can be scaled-up readily to produce large quantities (liters) of dispersions. At an initial concentration of 0.5 wt% and a grinding time 10 h we produced 250 mL of the dispersion in NMP (Figure S2) with a comparable concentration (0.3 wt%) and very high stability for a very long time period (> 6 month). This method has the advantage of allowing large volumes of dispersions to be prepared at once.

Figure S2. High yield of nanomaterials dispersion: Photograph of a high-quality dispersion of $NbSe_2$ in NMP (250 mL, 0.3 wt%).

S2 Sedimentation Tests:

We performed sedimentation tests by storing $NbSe_2$ dispersions (prepared with and without grinding) in NMP for more than six months. The material prepared without grinding precipitated completely after several minutes; in contrast, the dispersions of $NbSe_2$ nanosheets and nanorods were highly stable, without any precipitation. Thus, the grinding process increased the compatibility between the $NbSe_2$ nanomaterials and the organic solvent, increased the repulsive forces among the particles, and prevented the materials from undergoing serious aggregation.

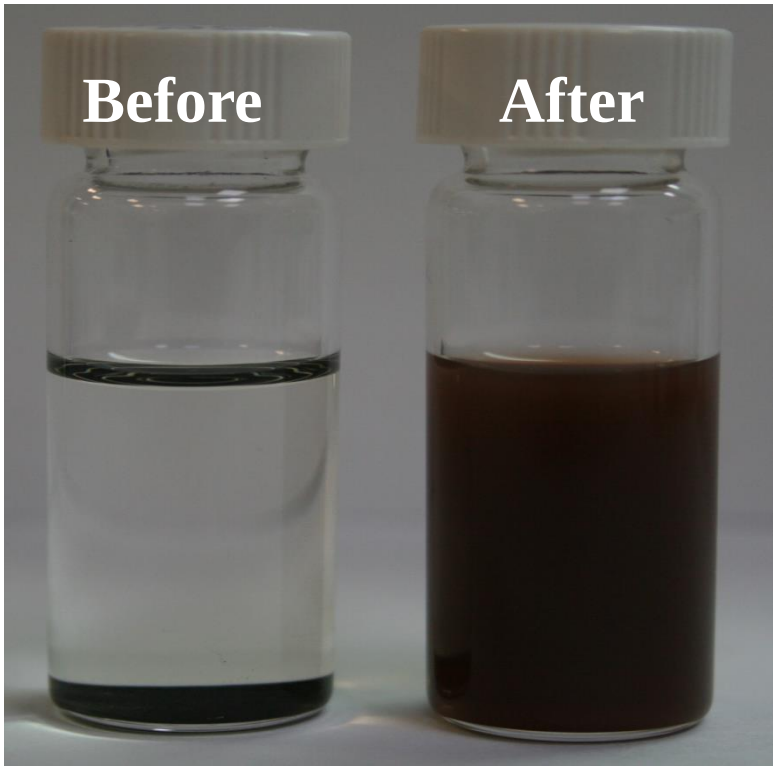

Figure S3. Sedimentation test: $NbSe_2$ dispersions (3 mL) before and after grinding for 10 h in NMP (starting concentration: 0.5 wt %). The dispersion prepared without grinding resulted in complete precipitation at the bottom of the vial within several minutes.

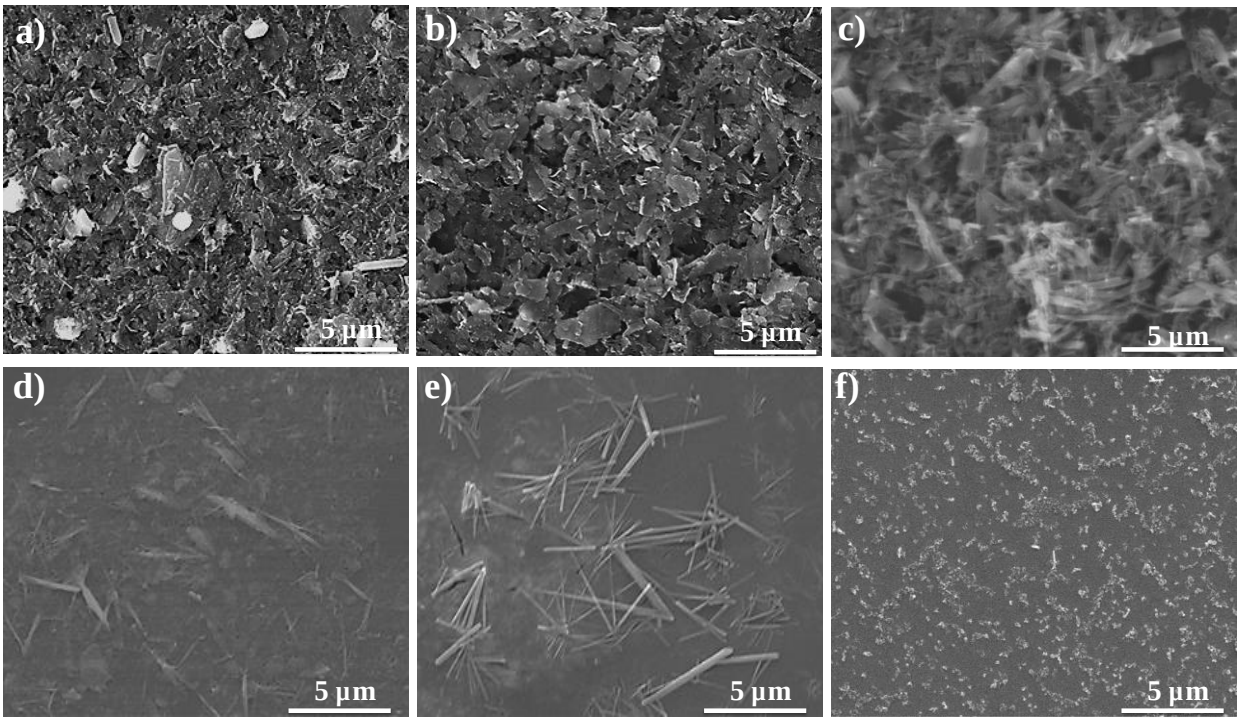

Figure S4. Morphologies of $NbSe_2$ materials during the conversion process: SEM images of the samples obtained at different time intervals during the conversion process from a 3D bulk $NbSe_2$ material into 2D nanosheets and then to 1D nanorods under the effect of mechanical forces: (**a**) pristine $NbSe_2$; after (**b**) 2, (**c**) 4, (**d**) 6, (**e**) 8, and (**f**) 10 h. Each dispersion was diluted tenfold with IPA and then drop-cast onto Si/SiO_2 and annealed (70 ℃, 10 min).

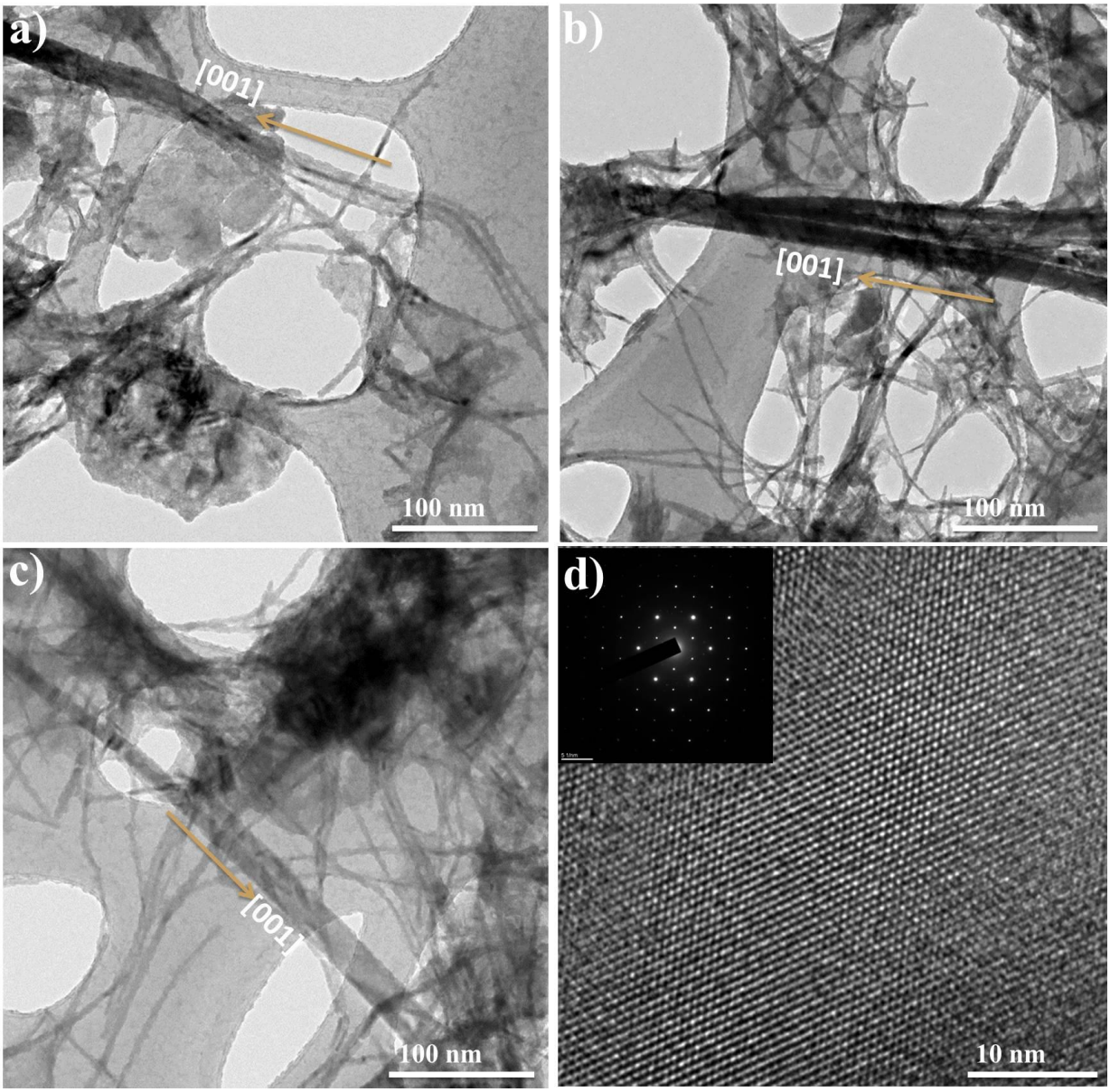

Figure S5. TEM analysis of fractured $NbSe_2$ nanostructures: (**a**, **b**, and **c**) TEM images for different fractured nanorods (the direction of fracturing showed with arrow) and (**d**) HRTEM image of flattened area of (**c**): The inset is the corresponding SAED of (**d**).

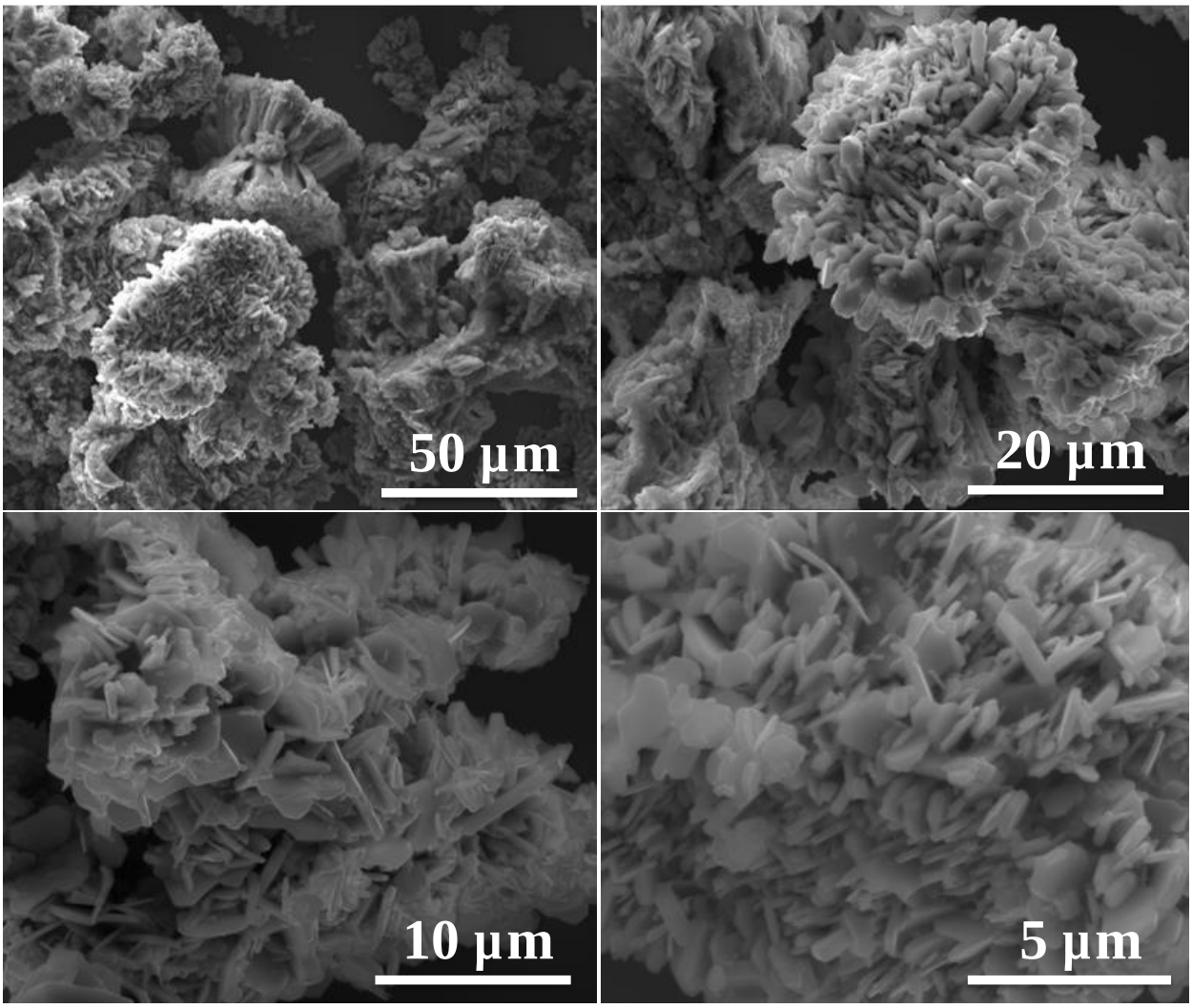

Figure S6. Morphology of pristine $NbSe_2$ materials: SEM images at different magnifications of the 3D network in the pristine $NbSe_2$ material, which consisted of a highly dense, layer-by-layer arrangements of single sheets with large lateral dimensions (>1 µm) and thicknesses of greater than 0.5 µm.

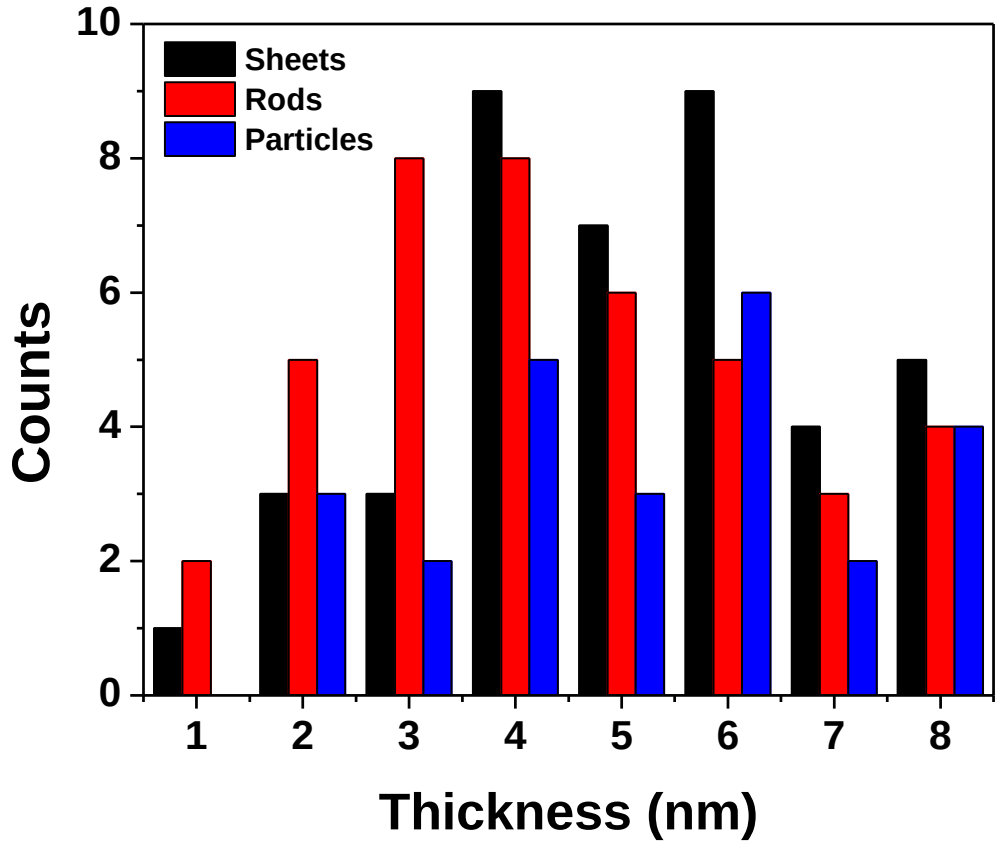

Figure S7. Histogram of $NbSe_2$ nanostructures: The thickness of the nanostructure from the height profile AFM images of 42 different nanosheets, 40 different nanorods, and 30 different nanoparticles. The average thicknesses approximately are 10, 5, and 3 nm for nanosheets, nanorods, and nanoparticles respectively.

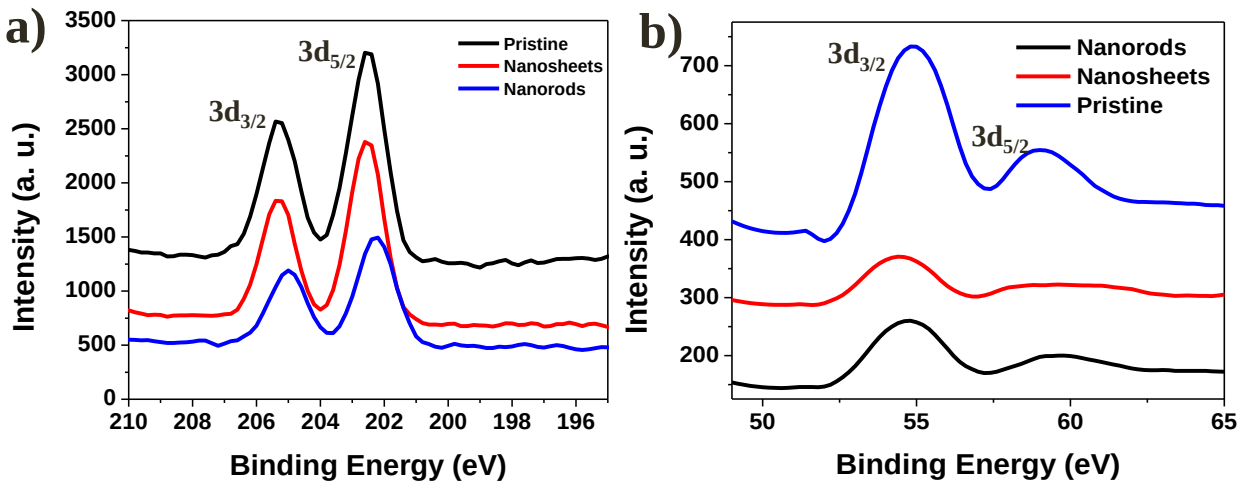

Figure S8. XPS analyses of $NbSe_2$ nanorods: XPS data of the binding energies of (**a**) Nb 3d and (**b**) Se 3d orbitals in $NbSe_2$ nanorod samples, prepared by placing drops of dispersions (diluted tenfold with IPA) onto Si/SiO_2 wafers and drying under an ambient atmosphere at 70 ℃ for 10 min. The peaks at 202.3 and 205.2 eV can be assigned to Nb $3d_{5/2}$ and Nb $3d_{3/2}$ orbitals, respectively; the peaks at 58 and 55.3 eV can be assigned to Se $3d_{5/2}$ and Se $3d_{3/2}$ orbitals, respectively. In addition, stoichiometry of niobium diselenide in the nanorods was confirmed from a Nb-to-Se atomic ratio of 1:2.

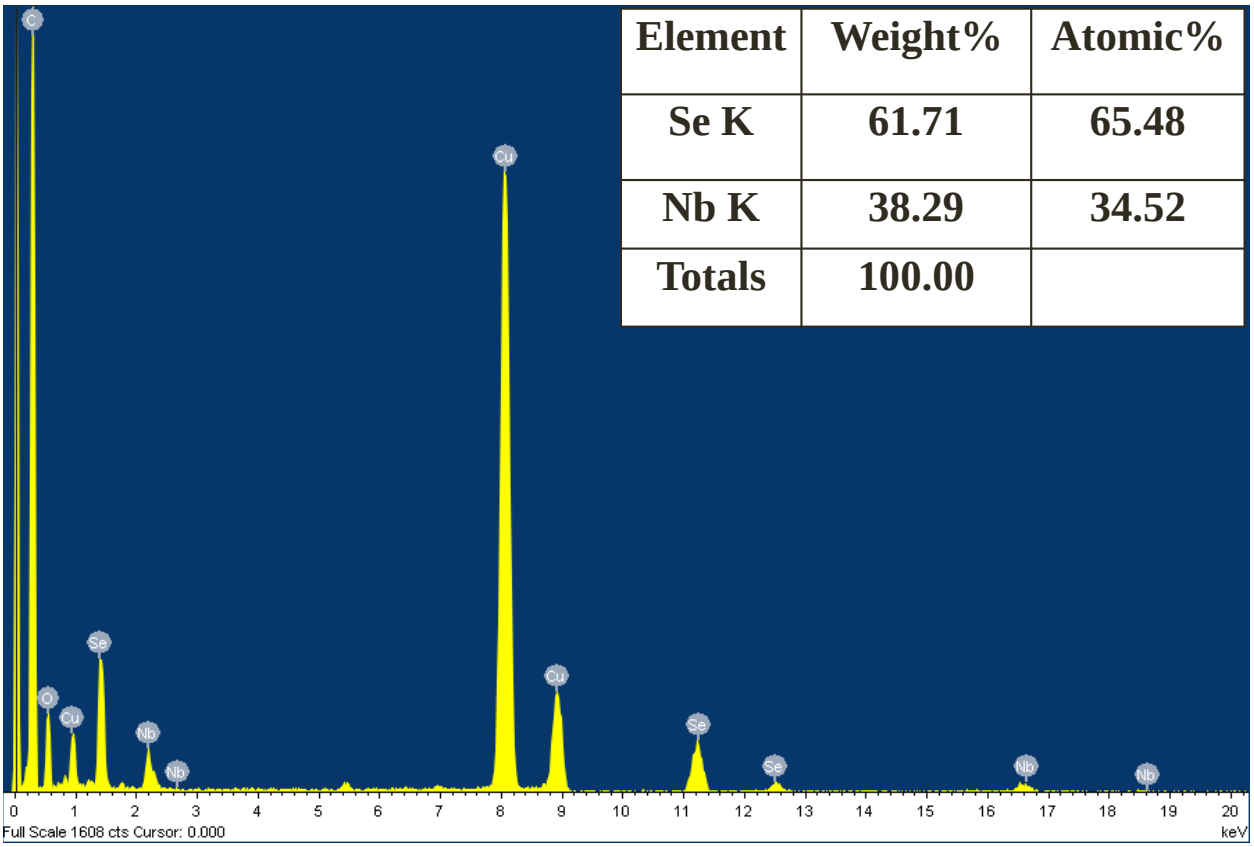

Element	Weight%	Atomic%
Se K	61.71	65.48
Nb K	38.29	34.52
Totals	100.00	

Figure S9. Compositional analysis of ultrathin $NbSe_2$ nanorods: Energy-dispersive X-ray analysis (EDS) of $NbSe_2$ nanorods revealing the atomic ratio of Nb-to-Se to be 1:1.9 (see inset Table), in agreement with the stoichiometric ratio of $NbSe_2$. Signals for copper atoms arose from the holey carbon-coated copper grid.

S3 Optical and Electrical Properties of thin films:

Both the transmittance (T) and sheet resistance (R_s) data of transparent conducting films are linked together and determined by the response of electrons to either static (voltage) or dynamic (light) electric fields. The relationship between them for a thin conducting film can be given by

$$T = \left[1 + \frac{Zo}{2Rs}\frac{\sigma_{OP}}{\sigma_{DC}}\right]^{-2} \quad \text{..... S1}$$

Where Z_0 is the impedance of free space and has the value 377 Ω. This relationship is controlled by the conductivity ratio, σ_{DC}/σ_{OP}, which can then be used as a Figure of Merit for transparent conducting films. It is well established that thick films give low values of T and high values of R_s, while thin films give high values of T and low values of R_s. The minimum industry standard for transparent conductors requires a value of σ_{DC}/σ_{OP} of 35 (giving T = 90% for R_s = 100 Ω/sq). For most current-driven applications, however, more stringent conditions (R_s < 10 @ T > 85%) are necessary.[2–4] For films of $NbSe_2$ nanosheets and rods (Figure S11), the values of σ_{DC}/σ_{OP} were approximately equal to 1. Accordingly, the $NbSe_2$ films on PET exhibited the properties of typical graphene networks, making such films promising materials for use as transparent conductors.

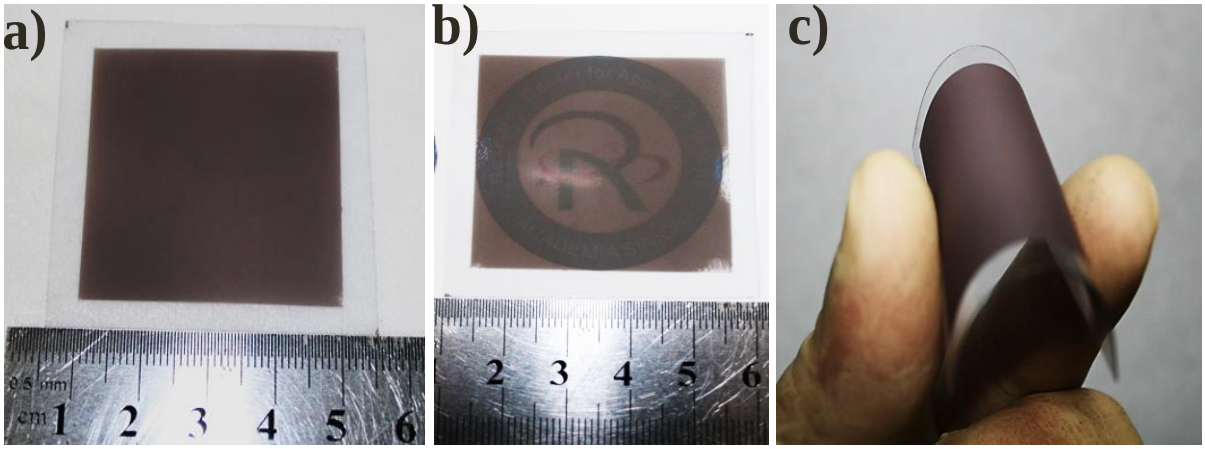

Figure S10. Large area thin film: Thin film of $NbSe_2$ prepared by spray-coating on a PET substrate. (**a**) 4 × 4 cm thin film; (**b**) semi-transparency of the film in (**a**); (**c**) flexibility of the thin film, with a bending angle of greater than 60°.

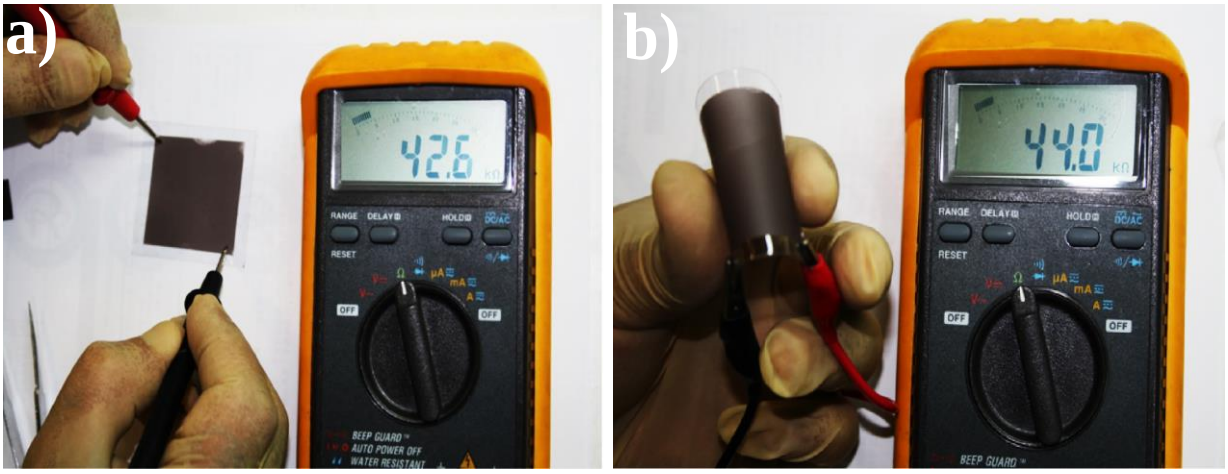

Figure S11. Bending tests of thin film: Resistance measurements of a large-area (4 × 4 cm) thin film of $NbSe_2$ prepared by spray-coating on a PET substrate. (**a**) Flat thin film; (**b**) thin film bent at an angle of greater than 60°. The resistance measured with an AVO meter, of the thin film before and after bending remained relatively constant (ca. 44 kΩ).

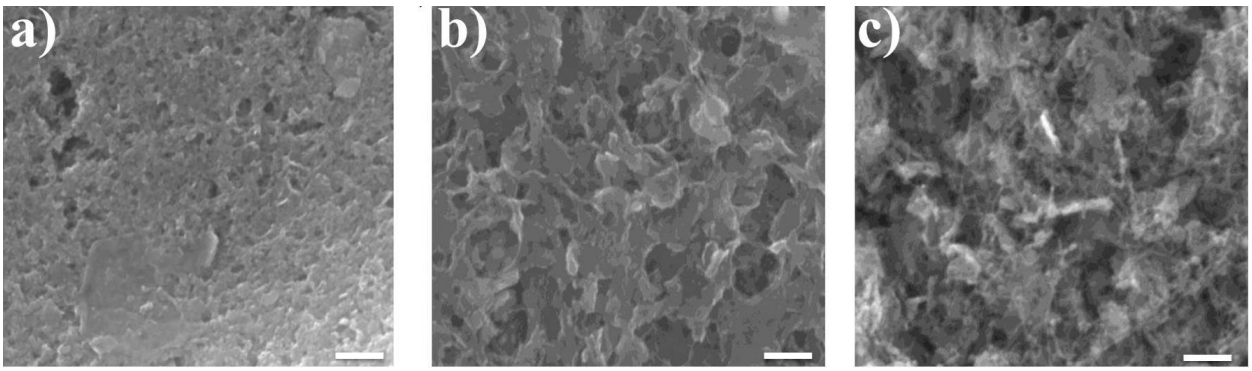

Figure S12. SEM images of $NbSe_2$ electrods (a) nanoparticles, (b) nanosheets, and (c) nanorods prepared on FTO substrates. The scal bare is 100 nm.

S4 Equipment and Experimental Conditions:

Mechanical comminuting through bead-milling in a homemade instrument was performed for different time intervals. The stirrer comprised three perforated discs mounted on a drive shaft (Sachem S1). The beads and the suspension were stirred by a central rotating agitator, typically at 1000–3000 rpm. The fluid rotation between the disc tip and the fixed wall of the mill generated an instability, driven by the centrifugal force, similar to Couette–Taylor instability occurring in the gap between two cylinders (the inner cylinder is rotating while the outer one stays at rest).[1] The apparent volume of grinding micronized beads was approximately 50%; the remaining volume was a suspension of the particles to be ground. The carrying fluid was an aqueous solution with grinding aids. Particle fragmentation resulted from the capture of particles inside zones subjected to the strong stress arising from two grinding beads colliding (frontal collisions in straining regions or oblique collisions induced by local shear). The comminution of the feed particles in a stirred media mill may occur through to two distinct mechanical phenomena: the particles are either squeezed between two colliding grinding beads or between a bead and a wall. The centrifugal force of the suspension was related to the tangential mean flow

induced by the high speeds of the rotating shaft and discs. Particles and beads in the vicinity of the outer wall of the mill chamber experienced a high pressure.

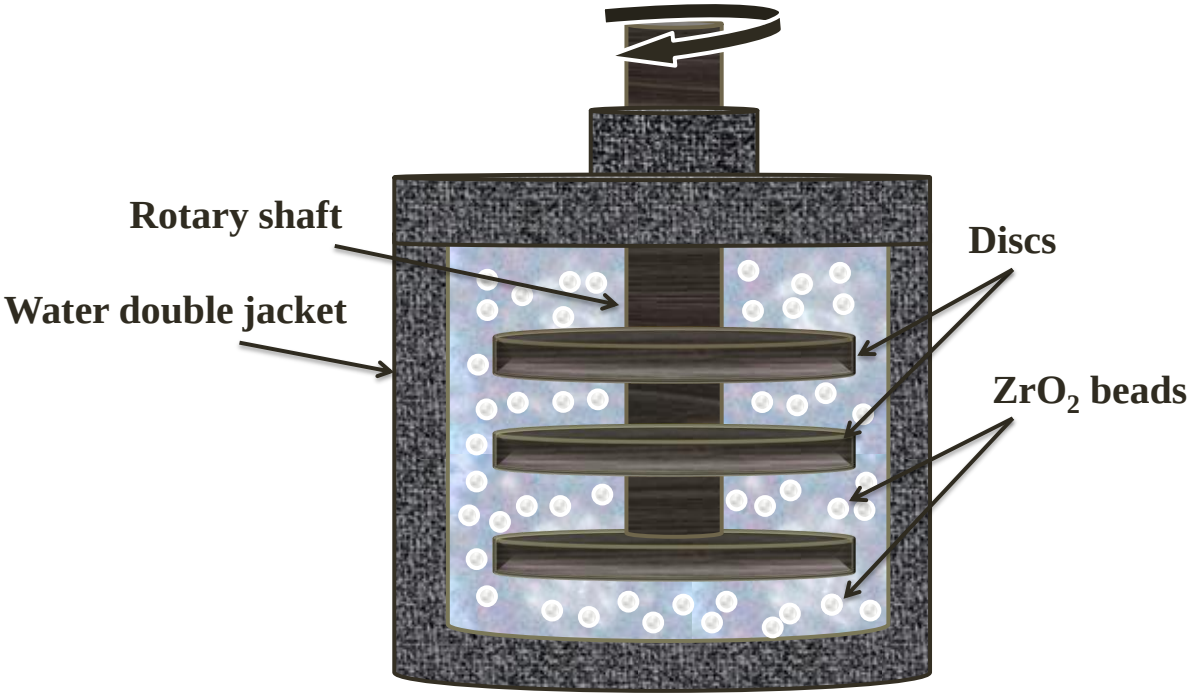

Scheme S1.Schematic representation of milling equipment: Schematic representation of the grinding machine; the apparent volume of the grinding beads was approximately 50%, with the remaining volume comprising a suspension of particles.

Supplementary References

1 Gers, R., Climent, E., Legendre, D., Anne-Archard, D. & Frances, C. *Chem Eng Sci* , 2010, **65**, 2052–2064

2 Smith, R. J. *et al. Adv Mater, 2011,* **23**, 3944–3948.

3 De, S. & Coleman, J. N. *ACS Nano, 2010*, **4**, 2713–2720.

4 Reynolds, K. J., Frey, G. L. & Friend, R. H. *Appl Phys Lett, 2033*, **82**, 1123–1125 (2003).